

EFFECT OF SUBSTRATE ORIENTATION AND HYDROGEN IMPURITIES ON FLUX PENETRATION IN Nb THIN FILMS

M. S. Welling, C. M. Aegerter, R. J. Wijngaarden, and R. Griessen
Vrije Universiteit Amsterdam, Faculty of Sciences, Division of Physics and Astronomy

Abstract: Very different kinds of magnetic flux penetration patterns have been reported in the type-II superconductor Nb. Using our advanced magneto-optical setup we investigate the flux penetration in Nb thin films. We find that depending on the sapphire substrate orientation (either A-plane or R-plane) qualitatively different structures are observed. In particular, for the A-plane orientation we find fingering and branching, whereas for R-plane samples a rough but continuous flux front is observed. Since Nb easily accepts hydrogen atoms as interstitial impurities, the influence of static pinning centers on the flux penetration process can be investigated. We find that the flux penetration drastically changes, becoming more irregular. The possibility to add a well-controlled amount of disorder makes NbH_x an ideal system to study the influence of quenched noise on roughening phenomena.

Key words: magneto-optical, niobium, flux penetration, hydrogen impurities, thermo-magnetic avalanches, Molecular-Beam Epitaxy

1 Introduction

Complex flux penetration patterns have been observed in type-II superconductors that are different from classical flux penetration behavior described by Bean [1]. For instance dendritic flux patterns triggered by local heating with a laser pulse are found in $\text{YBa}_2\text{Cu}_3\text{O}_{7-x}$ [2] from magneto-optical (MO) studies. Similar dendritic structures are also reported for MgB_2 [3].

For the low temperature superconductor niobium several authors found rather different magnetic flux patterns. Huebener *et al.* observe smooth structures in niobium foils whereas for sputtered thin films seaweed-like patterns are reported [4]. Other finger-like patterns are reported by Aoki and Habermeier [5] and also by Rowe *et al.* [6]. Studies by Duran *et al.* [7], who used sputtered Nb films on various kinds of substrates, revealed tree-like patterns, while James *et al.* [8] using scanning Hall probe microscopy found ‘rough’ Bean-like flux patterns.

The qualitatively different magnetic flux patterns in superconducting niobium arise supposedly because of differences in the defect structures of the investigated samples. Here we investigate the influence of hydrogen impurities on the flux penetration behavior since niobium easily absorbs hydrogen thereby changing the defect structure and destroying superconductivity on a local scale. We show that by increasing the hydrogen content (increase the amount of defects) we are able to change the flux penetration pattern. Since often niobium samples are grown on sapphire substrates, we restrict our experimental investigation to niobium films grown on A (11 $\bar{2}$ 0) and R (1102) sapphire substrates.

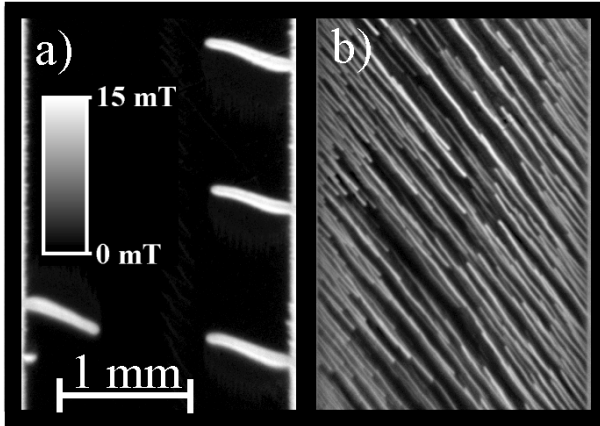


Figure 1. Measured local magnetic induction B_z in a 500 nm Nb thin film on an A-plane substrate after zero field cooling to 4.2 K and subsequently applying a field of 6.8 mT. (a) the as-grown film shows finger-like flux protrusions, which enter the sample in an abrupt manner. (b) shows the same film after exposure to hydrogen gas at a pressure of 60. The black area corresponds to the Meissner phase, and bright regions to the Shubnikov phase. The magnetic flux distribution shows easy flow channels.

2 Experimental details

In this section the sample, the MO set-up, the magnetic field sweep- and the hydrogenation- procedure are presented.

Nb thin films of thickness 500 nm are made by e-gun evaporating under Ultra High Vacuum (UHV) conditions (base pressure: $1 \cdot 10^{-7}$ Pa) on A-plane (11 $\bar{2}$ 0) and R-plane (1 $\bar{1}$ 02) sapphire substrates ($T_{sub} = 973$ K). Prior to evaporation the substrates are cleaned and subsequently baked out at 973 K. To obtain a strip geometry of 9.0×1.8 mm² we use a shadow mask. If niobium is exposed to air, a thin layer at the sample surface oxidizes, which is hardly permeable to hydrogen. To prevent this and to be able to introduce hydrogen into the films afterwards, a 10 nm thick Pd cap layer is evaporated *in-situ* on top of the Nb films at room temperature. Palladium catalytically dissociates the H₂ molecules into H atoms that diffuse easily into the niobium film. We estimate, from the hydrogen partial pressure, that the hydrogen contamination in the fabricated film less than 0.1 %.

We measure the local magnetic induction B_z directly above the superconducting sample using an MO set-up [9] by detecting the polarization change in a Bi-substituted ferrite-garnet film [10] with in-plane magnetization vector and large Faraday effect (typically 0.06 deg/mT). We mount this ‘indicator’ on top of the sample and place the assembly in our specially built cryogenic polarization microscope, which fits into the variable temperature insert of an Oxford Instruments 1-T magnet system. We use a small amount of helium gas (partial pressure $6 \cdot 10^3$ Pa) in the sample space for good thermal contact of the sample with the cryostat.

Our experiments are performed at 4.2 K after zero field cooling (ZFC). We apply the external magnetic field perpendicular to the sample and indicator surface and increase it from 0 to 20 mT in steps of 50 μ T, using a constant sweep rate of 50 μ T/s between steps. After every field step, the flux distribution in the sample is relaxed for 3 seconds after which an MO image is acquired. To avoid geometrical effects due to the corners, we investigate only the middle part of the sample. Our camera has 782×582 pixels and the exposure time is 300 ms. The spatial resolution is such that the width of a square pixel equals 3.4 μ m. Each experiment is repeated at least once to investigate reproducibility. After repeating the experiment we heat up the sample to room temperature. Next, the sample space is flushed with helium gas and the hydrogen content of the sample is increased by applying about twice the previously applied hydrogen pressure (further details below). Before cooling down again, we wait one hour (at room temperature) to equilibrate the hydrogen concentration throughout the sample.

3 Substrate orientation

We now discuss the role of the substrate orientation on the flux penetration pattern and show the rather different behavior observed for flux penetration in the as-grown niobium on either A- or R-plane sapphire.

In figure 1a we show the measured local magnetic induction B_z in a Nb thin film on an A-plane substrate at 6.8 mT after ZFC to 4.2 K. The scale-bar indicates the magnetic induction B_z . Note that the Meissner phase appears black and the Shubnikov phase bright. With increasing magnetic field, the flux suddenly starts to enter in finger-like bursts of magnetic flux, which appear instantaneously (our temporal resolution exceeds the time of formation). We observe the apparent presence of a repulsive interaction between neighboring fingers causing more complex meandering and branching of the fingers with increasing external field. Above ~ 6.2 K the finger-like protrusions of magnetic flux are absent and flux penetrates in a smoother way [11]. Our observations are consistent with the occurrence of thermo-magnetic avalanches proposed by Aranson *et al.* [12] where a hot spot starting at the edge moves into the superconductor causing branching of the penetrating flux when it encounters defects.

In figure 2a we show the measured local magnetic induction B_z in a Nb thin film on a R-plane substrate at 8.0 mT after ZFC to 4.2 K. Again the scale-bar indicates the magnetic induction B_z . Note however that now fingers are absent and the flux penetrates in a gradual manner without large avalanches. While slowly increasing the magnetic field, the flux appears to penetrate in small plumes forming a somewhat irregular ‘flux front’. The flux front is defined as the borderline between the Meissner and the Shubnikov phase. In the next section we investigate the role of hydrogen impurities on the flux penetration.

4 Hydrogen impurities

It is well known that Nb easily absorbs hydrogen. However, the influence of hydrogen on the superconducting properties [13] of Nb films has not been investigated in great detail. Most investigations concentrated on changes in electronic, magnetic, and structural properties of the NbH_x system. With increasing hydrogen concentration the niobium lattice expands [14] leading to morphological changes, crystal lattice distortions, and dislocations [15]. We now discuss the various different phases that can be expected to be formed based on the bulk phase diagram [16]. For low hydrogen

concentrations around room temperature (where we change the hydrogen concentration) the α phase is formed, which is a disordered solution of hydrogen in bcc niobium with low hydrogen concentration. At somewhat higher hydrogen concentrations the β phase is formed resulting in coexistence of $\alpha + \beta$ phases. The β phase is an ordered interstitial solid solution of hydrogen. It is important to note that the β phase is not superconducting above 1.2 K [16,17], while the lowest temperature investigated here is 4.2 K. Upon cooling down to 4.2 K the ϵ phase forms. Randomly distributed precipitates of ϵ phase with typical sub-micrometer size are formed. Thus at low temperature we expect the $\alpha + \epsilon$ phases with (at high hydrogen concentrations) β phase regions. We present now the results for the Nb films on A-plane substrates. The results of Nb films on R-plane substrates are given at the end of this section.

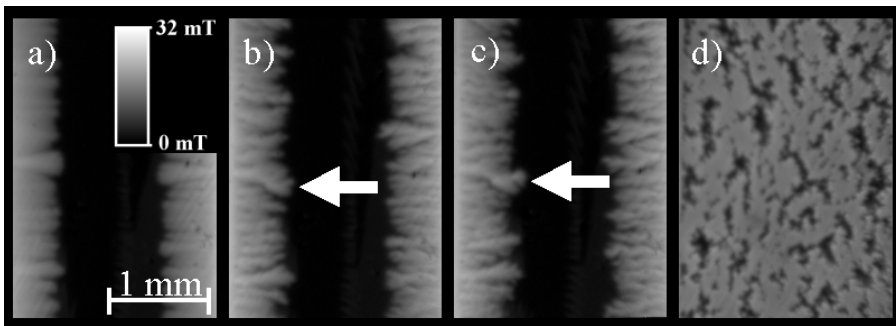


Figure 2. Measured local magnetic induction B_z in a 500 nm thick Nb thin film on a R-plane substrate after zero field cooling at 4.2 K and subsequently applying a field of 8.0 mT. Figures a to d show the same region after exposure to hydrogen gas pressures of 0, 80, 260, and 40000 Pa. The hydrogen gas pressure is changed at room temperature. After zero field cooling, the complete evolution of the magnetic flux penetration, with increasing the magnetic field, is obtained. The black area corresponds to the Meissner phase, and bright regions to the Shubnikov phase. The arrows in b and c indicate the growth of a branching magnetic flux protrusion with increasing hydrogen content. Fragmentation into superconducting islands is visible in figure d, see text for more details.

In figure 1b, we show the measured local magnetic induction B_z in a Nb film on an *A-plane substrate* after loading with hydrogen at a hydrogen gas pressure of 60 Pa at room temperature. The sample is ZFC to 4.2 K and subsequently a magnetic field of 6.8 mT is applied. Black areas correspond to the Meissner phase and bright regions to the Shubnikov phase. Figure 1a shows the sample *before* applying hydrogen. Note that in both cases the magnetic flux penetrates in a burst-like manner through channels, but these

are much narrower and more closely spaced in the sample containing hydrogen. Note also the change of direction of entering flux with increased hydrogen content. We suppose this is due to surface corrugation due to the Nb lattice expansion.

Figures 2a to 2d show the measured magnetic induction B_z in a Nb thin film on a *R-plane substrate* after ZFC to 4.2 K and subsequently applying a magnetic field of 8.0 mT. Figure 2a shows the flux penetration in the as-grown film together with a gray-scale bar indicating the local magnetic induction, which holds for all images. The hydrogen content of the sample is increased in figures 2b to 2d by applying a hydrogen gas pressure of 80, 260, and 40000 Pa at room temperature. Thus for every experiment the sample is increasingly loaded with hydrogen and after ZFC the complete evolution of the magnetic flux penetration, with increasing magnetic field, is obtained. Note that for figure 2a to 2c upon increasing the externally applied magnetic field vortices start to penetrate the superconductor from the edge. By increasing the hydrogen content the flux penetration becomes more irregular. For example, the arrows in figure 2b and 2c point at one magnetic flux protrusion which splits more and more with increasing hydrogen concentration. Note that the flux penetrates further into the superconductor with increasing hydrogen content indicating a decrease of the critical current. The formation of the β phase accompanied by loss of superconductivity can be observed in figure 2d. Obvious is the fragmentation of the superconductor in superconducting islands (black) that are now separately subjected to the externally applied magnetic field.

5 Summary

In conclusion, we presented MO measurements of the local magnetic induction B_z in Nb superconducting thin films on A- and R-plane sapphire substrates. We show by visualizing the changing of the flux penetration behavior that one can change the defect structure of the samples by increasing the hydrogen content.

Depending on the sapphire substrate orientation (either A-plane or R-plane) qualitatively different structures are observed in the ‘hydrogen free’ samples. For the A-plane orientation we find fingering and branching similar to what would be expected from large-scale thermo-magnetic avalanches [12]. Above ~ 6.2 K these large finger-like shape magnetic flux protrusions are absent. For the R-plane orientation, we find that flux penetration takes place in a gradual manner and large-scale thermo-magnetic avalanches are absent. Only a somewhat irregular ‘flux front’ (borderline between the Meissner and the Shubnikov phase) is formed upon increase of the externally applied magnetic field.

Because Nb easily accepts hydrogen atoms as interstitial impurities, even from hydrogen gas present in the atmosphere surrounding the sample or during evaporation one could expect differences in flux penetration behavior depending on hydrogen contamination. We showed that if hydrogen is applied after evaporation, only concentrations above 60 Pa significantly change the flux penetration, implying that the flux penetration is actually dominated by the defect structure already present in the as-grown films. Therefore the differences between flux patterns reported in literature are probably mainly caused by differences in defect structure.

Finally, the possibility to change the disorder in a well-controlled way (by hydrogen), allows us to study in a detailed way the influence of disorder on roughening phenomena [18,19].

Acknowledgements

We would like to thank Nico Koeman for providing the samples and Arndt Remhof for useful discussions. This work was supported by FOM (Stichting voor Fundamenteel Onderzoek der Materie), which is financially supported by NWO (Nederlandse Organisatie voor Wetenschappelijk Onderzoek). We also acknowledge the ESF (European Science Foundation) VORTEX Program for support.

References

- 1 C. P. Bean, *Rev. Mod. Phys.* **36**, 31 (1964).
- 2 V. Bujok, P. Brüll, J. Boneberg, S. Herminghaus, and P. Leiderer, *Appl. Phys. Lett.* **63**, 412 (1993).
- 3 T. H. Johansen, M. Baziljevich, D. V. Shantsev, P. E. Goa, Y. M. Galperin, W. N. Kang, H. J. Kim, E. M. Choi, M. S. Kim and S. I. Lee, *Europhys.Lett.* **59**, 599 (2002), A. V. Bobyl and D. V. Shantsev, T. H. Johansen, W. N. Kang, H. J. Kim, E. M. Choi, and S. I. Lee, *Appl. Phys. Lett.* **80**, 4588 (2002).
- 4 R. P. Huebener, V.A. Rowe, and R. T. Kampwirth, *J. Appl. Phys.* **41**, 2963 (1970).
- 5 R. Aoki and H. U. Habermeier, *Jpn. J. Appl. Phys.* **26**, 1453 (1987).
- 6 V. A. Rowe, R. P. Huebener, and R. T. Kampwirth, *Phys. Stat. Sol. (a)* **4**, 513 (1971).
- 7 C. A. Duran, P. L. Gammel, R. E. Miller, D. J. Bishop, *Phys. Rev. B* **52**, 75 (1995).
- 8 S. S. James, S. B. Field, J. Seigel and H. Shtrikman, *Physica C* **332**, 445 (2000).
- 9 R. J. Wijngaarden, K. Heeck, M. Welling, R. Limburg, M. Pannetier, K. van Zetten, V. L. G. Roorda, A. R. Voorwinden, *Rev. Sci. Instrum.* **72**, 2661 (2001).
- 10 L. A. Dorosinskii, M. V. Indenbom, V. I. Nikitenko, Y. A. Ossipyan, A. A. Polyanskii, V. K. Vlasko-Vlasov, *Physica C* **203**, 149 (1992).

- 11 M. S. Welling and R. J. Wijngaarden to be published.
- 12 I. Aranson, A. Gurevich, V. Vinokur, Phys. Rev. Lett. **87**, 067003 (2001).
- 13 L. Ya. Vinnikov, O. V. Zharikov, Ch. V. Kopetskii, and V. M. Polovov, Sov. J. Low Temp. Phys. **3**, 4 (1977).
- 14 G. Song, A. Remhof, D. Laberge, and H. Zabel, Phys. Rev. B **66**, 045407 (2002). G. Song, A. Remhof, K. Theis-Bröhl, and H. Zabel, Phys. Rev. Lett. **79**, 5062 (1997). G. Song, M. Geitz, A. Abromeit, and H. Zabel, Phys. Rev. B **54**, 14093 (1996).
- 15 C. P. Herring, J. Phys. F: Metal Phys. **6**, 99 (1976).
- 16 G. Alefeld and J. Völkl, Hydrogen in Metals II, Topics in applied Physics volume 29, Springer Verlag.
- 17 J. M. Welter, and F. J. Johnen, Z. Physik B **27**, 227 (1977).
- 18 R. Surdeanu, R. J. Wijngaarden, E. Visser, J. M. Huijbregtse, J. H. Rector, B. Dam, and R. Griessen, Phys. Rev. Lett. **83**, 2054 (1999).
- 19 M. S. Welling, C. M. Aegerter and R. J. Wijngaarden, Europhys. Lett. **61**, 473 (2003).